Acta Biochim Biophys Sin 2022, 54(9): 1376–1385
https://doi.org/10.3724/abbs.2022125
Advance Access Publication Date: 15 September 2022
Original Article

Original Article

Exploration and validation of a novel ferroptosis-related gene signature predicting the prognosis of intrahepatic cholangiocarcinoma

Xinfei Yao[1,†], Bo Chen[4,†], Mingxun Wang[2,†], Sina Zhang[4], Bangjie He[4], Zhehao Shi[4], Tuo Deng[4], Wenming Bao[4], Yi Wang[3], Gang Chen[4,5,*], and Zhiyuan Bo[4,5,*]

[1]The First Clinical College, Wenzhou Medical University, Wenzhou 325035, China, [2]Department of Ultrasonography, The First Affiliated Hospital of Wenzhou Medical University, Wenzhou 325035, China, [3]Department of Epidemiology and Biostatistics, School of Public Health and Management, Wenzhou Medical University, Wenzhou 325035, China, [4]Department of Hepatobiliary Surgery, The First Affiliated Hospital of Wenzhou Medical University, Wenzhou 325035, China, and [5]Key Laboratory of Diagnosis and Treatment of Severe Hepato-Pancreatic Diseases of Zhejiang Province, The First Affiliated Hospital of Wenzhou Medical University, Wenzhou 325035, China

[†]These authors contributed equally to this work.

*Correspondence address. Tel: +86-577-55579453; E-mail: drbozhiyuan@163.com (Z.B.) / Tel +86-577-55579453; E-mail: chen.gang@wmu.edu.cn (G.C.)

Received 02 April 2022 Accepted 10 June 2022

Abstract

Ferroptosis plays an important role in intrahepatic cholangiocarcinoma (ICC). We aim to develop a new ferroptosis-related gene signature predicting the prognosis of ICC. We download RNA expression profiles and clinical data of ICC from TCGA and GEO databases. Ferroptosis-related differentially expressed genes (DEGs) are screened by the Wilcoxon signed-rank test. GO and KEGG enrichment analyses are performed to understand the function of DEGs and co-expressed genes. Univariate Cox and LASSO regression are used to develop a ferroptosis-related gene signature. Receiver operating characteristic (ROC) curves and Kaplan-Meier (KM) analysis were used to evaluate the prognostic value. RNA sequencing is performed in 30 patients with ICC in our medical center to validate the prognostic value of the gene signature. We identify 44 ferroptosis-related DEGs, among which four (ACSL4, IREB2, NFE2L2, and TP53) are associated with overall survival (OS). Functional enrichment analysis shows that ferroptosis-associated DEGs have an important impact on ICC carcinogenesis. A new ferroptosis-related gene signature based on DEGs is built, and the prognostic ability is confirmed by KM and ROC curves (AUC = 0.777, 0.75, 0.799 for 12, 24, and 36 months, respectively). Patients with high risk scores have worse OS (P = 0.0081). In the validation cohort, the expression of DEGs is in accordance with that in the exploration cohort. The four-gene signature is also demonstrated to have a favorable prognostic value (AUC = 0.69). A new predictive model based on four ferroptosis-related genes (ACSL4, IREB2, NFE2L2, and TP53) is established and shows favorable prognostic value.

Key words ferroptosis, intrahepatic cholangiocarcinoma, prognosis, gene signature

Introduction

Intrahepatic cholangiocarcinoma (ICC) is a rare malignancy originated from the bile duct [1]. As the most common primary biliary cancer, the incidence and mortality of ICC have gradually risen worldwide in recent years [2]. Owing to the difficulty in early diagnosis and highly aggressive nature, ICC has a poor prognosis [3]. Although radical surgery is the most effective treatment for ICC, it is only applicable in a small proportion of patients at first diagnosis. Even after liver resection, the median postoperative survival is approximately 26 months, with a high rate of tumor recurrence [4]. Therefore, an early reliable prognostic model for ICC is urgently needed to optimize the treatment scheme and to predict the prognosis of ICC.

A number of gene mutations, such as inhibitors targeting isocitrate dehydrogenase (IDH)-1 or -2 and fibroblast growth factor receptor (FGFR) fusions, have been identified in ICC, but these mutations only account for 10%–20% of ICC [5]. As a new form of programmed cell death, ferroptosis was first proposed in 2012 by

Dixon *et al.* [6]. It is marked by the excessive accumulation of iron, which can lead to lethal levels of lipid peroxidation. Many studies have shown that cancer cells need more iron to support growth than normal cells. In addition, the dependence on iron also makes cancer cells more susceptible to ferroptosis [7]. Ferroptosis has been found to play an important role in the development and progression of many malignant tumors, especially in tumors with a high propensity for metastasis and resistance to conventional therapies [8]. Ferroptosis may be a potential therapeutic target in the field of oncology. In addition to morphological features and biochemical features [9], many genes have been reported to regulate ferroptosis, such as acyl-CoA synthetase long-chain family member 4 (ACSL4) and nuclear factor erythroid 2-related factor 2 (NRF2) [10,11]. Although studies have shown the potential role of ferroptosis in a large variety of tumors (such as lung cancer, colorectal cancer and ovarian cancer), research on the role of ferroptosis in ICC remains lacking. Therefore, it is interesting to identify effective ferroptosis-related biomarkers to diagnose ICC patients at an early stage, evaluate the prognosis of ICC patients, and provide possible targeted therapy.

In this study, we aimed to explore the prognostic value of ferroptosis-related genes and develop a new prognostic risk model based on ferroptosis-related genes for ICC. We first analysed the RNA profiles and clinical information of ICC patients from The Cancer Genome Atlas (TCGA) and Gene Expression Omnibus (GEO) datasets. Then, we utilized the differentially expressed ferroptosis-related genes associated with overall survival (OS) to establish a new prognostic model. Finally, the results obtained from the exploratory cohorts were further verified in the Wenzhou Medical University (WMU) cohort. Through RNA sequencing of ICC in our medical center, the prognostic role and clinical value of the ferroptosis-related gene model were validated. This may provide new insight into the prediction and treatment of ICC.

Materials and Methods

Data collection

Level 3 RNA sequencing data and relevant clinical information were obtained from the TCGA database (https://portal.gdc.cancer.gov/repository) and GEO database (https://www.ncbi.nlm.nih.gov/geo/). The "Limma" R package was used to standardize the gene expression profiles. These data retrieved from the public database were used to build the exploration cohort. Our study adheres to the access policies and publication guidelines of the TCGA and GEO databases. We obtained 60 ferroptosis-associated genes from the previous literature [12–15], and 59 genes expressed in the ICC RNA-sequence were ultimately included.

Construction of the WMU cohort

To build the validation cohort, tumor tissues and tumor adjacent tissue were collected from 30 ICC patients who underwent surgery at the First Affiliated Hospital of Wenzhou Medical University between October 2017 and November 2019. All patients were pathologically diagnosed with primary ICC. The clinical information and follow-up information were obtained, and informed consent was also obtained from each patient before surgery. Then, the RNA expression data of the ICC were obtained by using transcriptional RNA sequencing. This trial was approved by the Ethics Committee of Wenzhou Medical University (2020-07) and adhered to the Declaration of Helsinki.

Identification of ferroptosis-related differentially expressed genes (DEGs)

We used the "Limma" R package to identify ferroptosis-related DEGs between tumor tissue and tumor adjacent tissue from TCGA and GEO databases. The Wilcoxon signed-rank test was used for the analysis of DEGs, and we set a threshold of false discovery rate (FDR) value < 0.05.

Functional annotation of DEGs

A protein-protein interaction (PPI) network for the overlapping ferroptosis-related DEGs was generated by the STRING database (https://string-db.org/). Furthermore, we also performed Gene Ontology (GO) and Kyoto Encyclopedia of Genes and Genomes (KEGG) pathway analyses using the "clusterProfiler" R package to further evaluate the potential value of ferroptosis-related genes for ICC. $P < 0.05$ was considered statistically significant.

Establishment and validation of a ferroptosis-related gene signature predicting the prognosis of ICC

Univariate Cox regression analysis was used to screen ferroptosis-related genes which were associated with the OS of ICC patients in the TCGA and GEO cohorts. Then, least absolute shrinkage and selection operator (LASSO) regression analysis was performed to prevent overfitting and construct a gene signature. Based on the gene signature, the risk score for each patient was calculated using the following formula: risk score = $e^{\text{sum(expression level of each gene} \times \text{corresponding coefficient)}}$. The patients were divided into high-risk and low-risk groups according to the median risk score. To evaluate the predictive value of the model, we used the "Survival ROC" R package to perform Kaplan-Meier (KM) survival curve analysis and time-dependent receiver operating characteristic (ROC) curve analysis. Furthermore, ICC patients with complete clinical predictors were enrolled to explore the independence of the ferroptosis-related signature, and univariate and multivariate Cox regression analyses were implemented.

Validation of the ferroptosis-related gene signature in the WMU cohort

Transcriptome sequencing analysis was used to acquire the RNA expression data from the collected samples. Total RNA was extracted from frozen tissue using TRIzol reagent (Life Technologies, Carlsbad, USA). Paired-end sequencing (2 × 100 bp) was performed using a BGI-500 instrument (BGI, Shenzhen, China) with a minimum of 20 million reads per sample. Sequencing data were processed and mapped to the human reference genome (hg19) using Bowtie2. Gene expression from sequencing was mapped by Per-Kilobase per Million mapped (RSEM) using fragments per kilobase per million (RPKM). The expression levels of four genes (*ACSL4*, *IREB2*, *NFE2L2*, and *TP53*) were validated in the WMU cohort. According to the formula of the gene signature above, the risk score of each patient was calculated, and KM curve and ROC curve analysis were also used to evaluate the predictive value of the gene signature in the WMU cohort.

Statistical analysis

R software (version 3.5.3) was used to perform the statistical analysis. The gene expression differences were analyzed through the

Wilcoxon signed-rank test. The chi-square test was used to compare categorical variables. Univariate Cox regression, multivariate Cox regression and LASSO regression were used to identify OS-related DEGs and clinical predictors. KM analysis and ROC curve analysis were used to evaluate the predictive value. Statistical significance was established at $P < 0.05$.

Results

Basic information

The flowchart of the study is shown in Figure 1. A total of 30 ICC patients (including 30 tumor samples and 9 tumor adjacent tissues) from TCGA database and 30 patients (including 30 tumor samples and 27 tumor adjacent tissues) from GEO database were enrolled in the exploratory cohort. Another 30 patients (including 30 tumor samples and 30 tumor adjacent tissues) who underwent radical surgery in our hospital were included in the WMU cohort as the validation cohort. Exact clinical data are shown in Table 1. The 1-, 2-, and 3-year OS rates of patients in the exploratory cohort were 82.5%, 63.4%, and 46.8%, respectively, and the 1-, 2- and 3-year disease-free survival (DFS) rates were 55.1%, 35.6%, and 35.6%, respectively. For the validation cohort, the 1-, 2-, and 3-year OS rates were 78.7%, 78.7%, and 45.6%, respectively.

Identification of ferroptosis-related DEGs in TCGA and GEO cohorts

By analyzing the 59 ferroptosis-related genes obtained from the previous literature, we identified 46 ferroptosis-related DEGs (35 upregulated genes and 11 downregulated genes) in the TCGA cohort and 53 DEGs (39 upregulated genes and 14 downregulated genes) in the GEO cohort (Figure 2A,C). Thus, 34 common unregulated and 10 common downregulated ferroptosis-related DEGs were screened (Figure 2B,D). The expression levels of 44 common DEGs in the TCGA and GEO integrated databases are shown in Figure 2E.

Functional annotation of ferroptosis-related DEGs

The PPI network of ferroptosis-related DEGs is shown in Figure 3A. The correlation networks of ferroptosis-related DEGs in the TCGA and GEO cohorts are presented in Figure 3B,C. Based on the results of GO function enrichment analyses, we found that ferroptosis-related DEGs are mainly associated with response to oxidative stress, cellular response to oxidative stress, cellular response to chemical stress, glutathione biosynthetic process, nonribosomal peptide biosynthetic process, sulfur compound biosynthetic process and iron ion homeostasis (Figure 3D,E). The KEGG enrichment analyses revealed that DEGs are significantly enriched in ferroptosis, ubiquitin-mediated proteolysis, central carbon metabolism in cancer, fatty acid biosynthesis and 2-oxocarboxylic acid metabolism according to the five top terms (Figure 3F,G). All these results indicated that ferroptosis-related DEGs play an important role in ICC initiation and development.

Construction of four ferroptosis-related gene signature predicting prognosis

In the TCGA and GEO cohorts, four ferroptosis-related DEGs (*ACSL4*, *IREB2*, *NFE2L2*, and *TP53*) were found to be associated with OS based on the results of univariate Cox regression (Figure 4A). Then, LASSO regression analysis was performed to develop the four-gene signature (Figure 4B,C). The patients were divided into a high-risk group ($n = 30$) and a low-risk group ($n = 30$) according to the median cut-off value (Figure 5D). The survival time of patients in the high-risk group was visibly shorter than that in the low-risk group (median OS: 64.6 months in the low-risk group and 24.3 months in the high-risk group) (Figure 5C). The 1-, 2-, and 3-

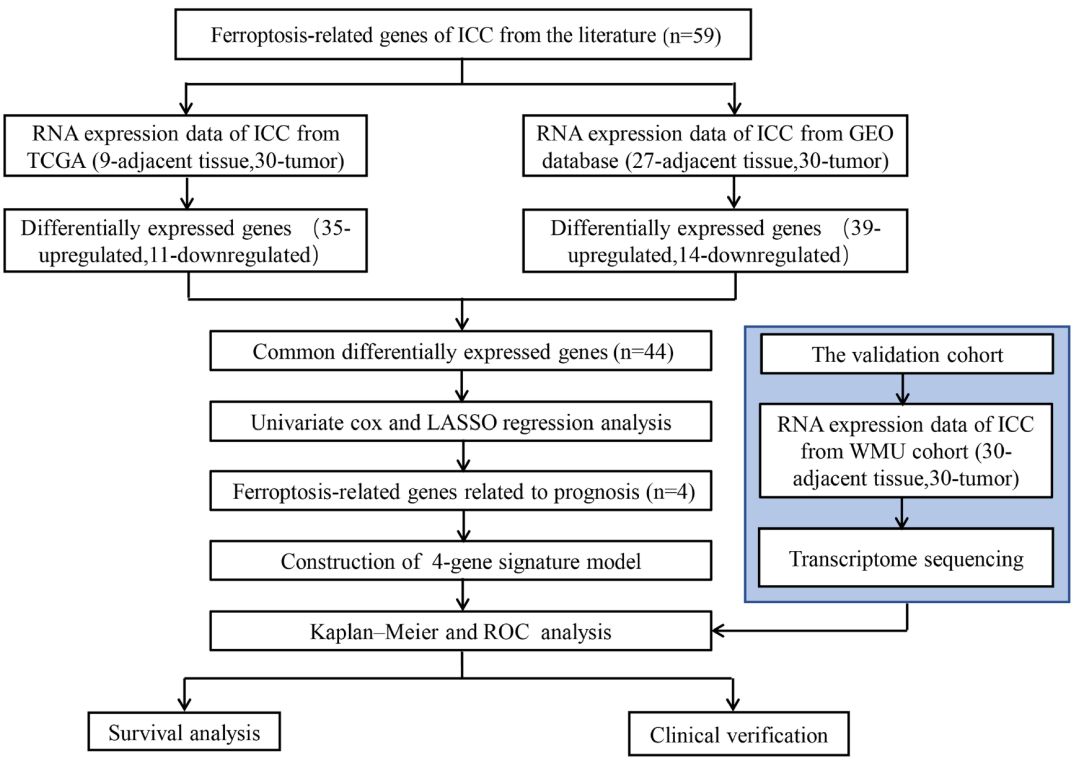

Figure 1. The flowchart of this study

Table 1. Clinical information of ICC patients from TCGA, GEO and WMU cohort

	TCGA cohort	GEO cohort	WMU cohort
Number of patients	30	30	30
Age (Median, Range)	64 (29,82)	65 (49,79)	65 (41,78)
Gender (%)			
Female	15 (50.0%)	6 (20.0%)	19 (63.3%)
Male	15 (50.0%)	24 (80.0%)	11 (36.7%)
Vascular invasion (%)			
No	25 (83.3%)	NA	22 (73.3%)
Yes	5 (16.7%)	NA	8 (26.7%)
Recurrence (%)			
Yes	15 (50.0%)	21 (70.0%)	19 (63.3%)
No	12 (40.0%)	9 (30.0%)	11 (36.7%)
unknown	3 (10.0%)	0 (0.00%)	0 (0.00%)
Stage (%)			
I	18 (60.0%)	NA	20 (66.7%)
II	8 (26.7%)	NA	6 (20.0%)
III	0 (0.00%)	NA	4 (13.3%)
IV	4 (13.3%)	NA	0 (0.00%)
Child-Pugh (%)			
A	16 (53.3%)	12 (40.0%)	29 (96.7%)
B	1 (3.33%)	18 (60.0%)	1 (3.33%)
C	0 (0.00%)	0 (0.00%)	0 (0.00%)
unknown	13 (43.3%)	0 (0.0%)	0 (0.0%)
Grade (%)			
G1	0 (0.00%)	NA	4 (13.3%)
G2	14 (46.7%)	NA	15 (50.0%)
G3	14 (46.7%)	NA	11 (36.7%)

year OS rates were 93.1%, 77.3%, and 67.0% in the low-risk group and 72.4%, 50.80%, and 28.20% in the high-risk group, respectively. K-M curve analysis showed that patients in the high-risk group had a worse OS ($P = 0.0081$, Figure 5A). Time-dependent ROC curves were used to evaluate the predictive value of the gene signature, and the areas under the curve (AUCs) were 0.777, 0.75, and 0.799 at 12 months,24 months, and 36 months, respectively (Figure 5B). To further understand the prognostic value of the four-gene signature in ICC, we compared DFS time in the high-risk (median DFS: 57.5 months) and low-risk groups (median DFS: 9.6 months), and the K-M curve of DFS indicated that the patients in the low-risk group had favorable DFS ($P = 0.02$, Supplementary Figure S1). The 1-, 2-, and 3-year DFS rates were 65.3%, 53.9%, and 53.9% in the low-risk group and 46.2%, 17.6%, and 17.6% in the high-risk group, respectively. The expression levels of ACSL4, IREB2, NFE2L2, and TP53 in both the low- and high-risk groups in the exploration cohort are shown in Figure 5E.

Validation of the independent prognostic value of the gene signature

Age, sex, grade, and stage were included in the survival analysis. The results of univariate Cox regression (HR = 2.625, 95% CI = 1.236–5.577, $p = 0.0312$) and multivariate Cox regression (HR = 3.147, 95% CI = 1.419–6.980, $P = 0.005$) showed that the four-gene signature is an independent prognostic factor affecting OS (Figure 6A,B).

Validation of four ferroptosis-related gene signature in the WMU cohort

The RNA expression data were extracted from the WMU cohort by transcriptome sequencing analysis. All four ferroptosis-related DEGs were upregulated in tumor tissue compared with tumor adjacent tissue in the WMU cohort (Figure 7I–L). The results were in accordance with the results from the TCGA cohort (Figure 7A–D) and the GEO cohort (Figure 7E–H). The patients were divided into a high-risk group ($n = 15$) and a low-risk group ($n = 15$) according to the median risk score calculated by the four-gene signature (Figure 6E). The survival time of patients in the high-risk group was obviously shorter t han that in the low-risk group (Figure 6F), and the 1-, 2-, and 3-year DFS rates were 93.3%, 93.3%, and 59.3% in the low-risk group and 61.5%, 61.5%, and 30.8% in the high-risk group, respectively. Kaplan–Meier curve analysis showed that patients in the high-risk group had a worse OS ($P = 0.059$, Figure 6C). Time-dependent ROC curves were generated, and the AUC of the ROC curve was 0.69 (Figure 6D). The expression levels of ACSL4, IREB2, NFE2L2, and TP53 in both the low- and high-risk groups in the WMU cohort are shown in Figure 6G.

Discussion

In recent years, ferroptosis has attracted much interest in the field of

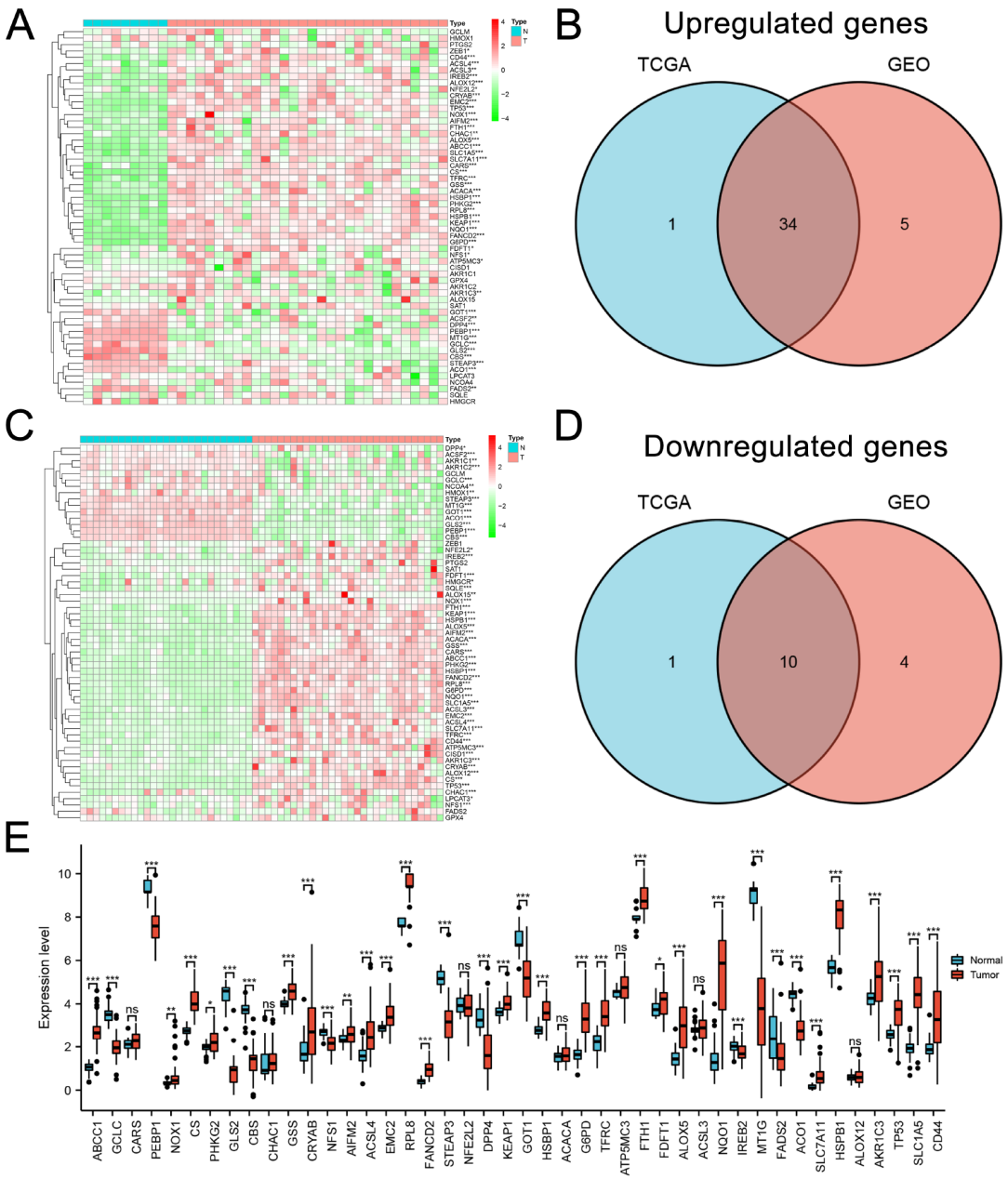

Figure 2. Identification of ferroptosis-related DEGs in TCGA and GEO cohorts (A,C) The heat-maps show the expression of 59 ferroptosis-associated genes in TCGA and GEO cohort. (B,D) Venn diagram shows the intersection of ferroptosis-related DEGs between TCGA and GEO cohort. (E) The expression levels of 44 common DEGs in the TCGA and GEO integrated database. $^{*}P<0.05$, $^{**}P<0.01$, $^{***}P<0.001$.

oncology [16–19]. Liu *et al.* [20] established a novel prognostic classifier based on ferroptosis and immune status in HCC. Li *et al.* [21] demonstrated the predictive application of ferroptosis-related genes for cholangiocarcinoma. However, few studies have reported the prognostic value of ferroptosis-related genes for ICC. To the best of our knowledge, this is the first study attempting to establish a new ferroptosis-related gene prognostic model for ICC and to further validate the predictive value in a clinical cohort.

In our study, we focused on identifying ferroptosis-related genes in ICC from public databases and our own database. By searching the previous literature, we obtained 59 ferroptosis-related genes. By screening the TCGA and GEO databases, we found 44 genes differentially expressed between the tumor tissue and tumor adjacent tissue. In addition, functional analyses showed that ferroptosis-associated genes have an important influence on the development and progression of ICC. Then, we tried to identify ferroptosis-related genes associated with prognosis by univariate Cox regression and LASSO regression analysis. Finally, we developed four ferroptosis-related DEGs (*ACSL4*, *IREB2*, *NFE2L2*, and *TP53*) to construct a gene signature model to predict the prognosis of ICC patients, and the performance of the signature was validated in the WMU cohort. All four ferroptosis-related DEGs were significantly upregulated in tumor tissue compared with tumor adjacent tissue in the TCGA, GEO, and WMU cohorts.

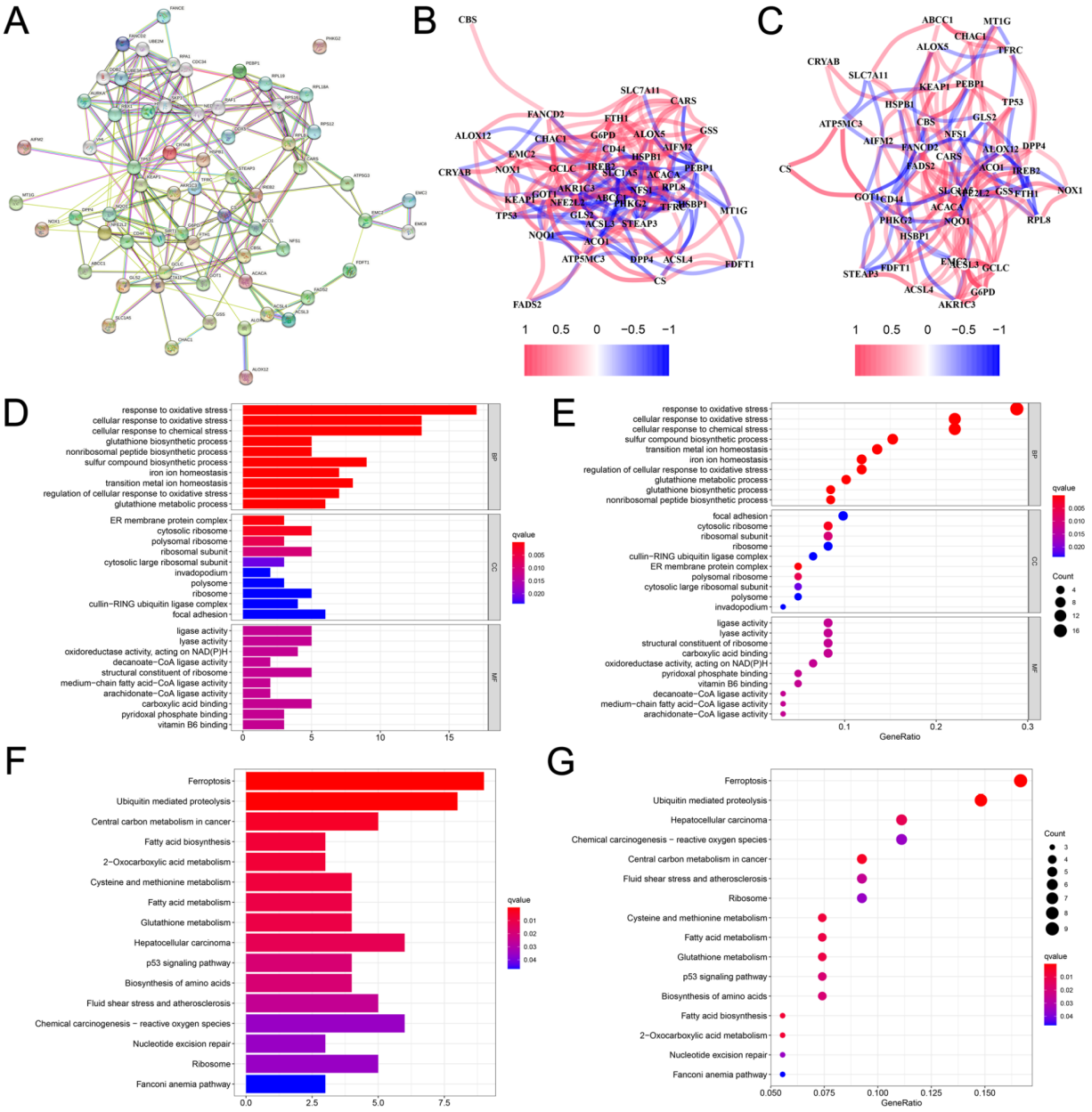

Figure 3. Functional annotation of ferroptosis-related DEGs (A)The PPI network of ferroptosis-related DEGs. (B) The correlation network of ferroptosis-related DEGs in TCGA cohort. (C) The correlation network of ferroptosis-related DEGs in GEO cohort. (D,E) The analysis of most significant GO function enrichment. (F,G) The analysis of most significant KEGG pathways.

Regarding the role of the four ferroptosis-related DEGs found in our study, *ACSL4* was demonstrated to be an important component promoting ferroptosis in a previous study [10]. As a promising prognostic biomarker, tumor ACSL4 is correlated with immune infiltration in cancers, and targeting ACSL4 may be a potential anticancer treatment [22,23]. In our study, high expression of ACSL4 in tumor tissue was found to be associated with a worse prognosis of ICC. IREB2 is a common ferroptosis-related gene, and inhibiting IREB2 notably weakens ferroptosis in non-small cell lung cancer, which leads to reduced antitumor efficiency [24]. The results obtained from our study also proved that IREB2 is a protective factor for ICC. Higher expression of IREB2 in tumor tissue is associated with better OS. NFE2L2 plays an important role in regulating ferroptosis and is a promising target for treatment of neurodegenerative diseases [25]. In a previous study performed by Yi *et al.* [26], NFE2L2 was identified as a low-risk gene in bladder cancer. This is in accordance with the results in our study of ICC. We found that high expression of NFE2L2 is associated with a better prognosis in ICC. TP53 plays a dual role in ferroptosis in various tumors through different mechanisms [27] and has also been identified as a prognostic factor and a potential therapeutic target. In our study, TP53 was demonstrated to be a protective factor with higher expression in tumor tissue. In summary, these four genes play an important role in ferroptosis and are closely associated with the prognosis of

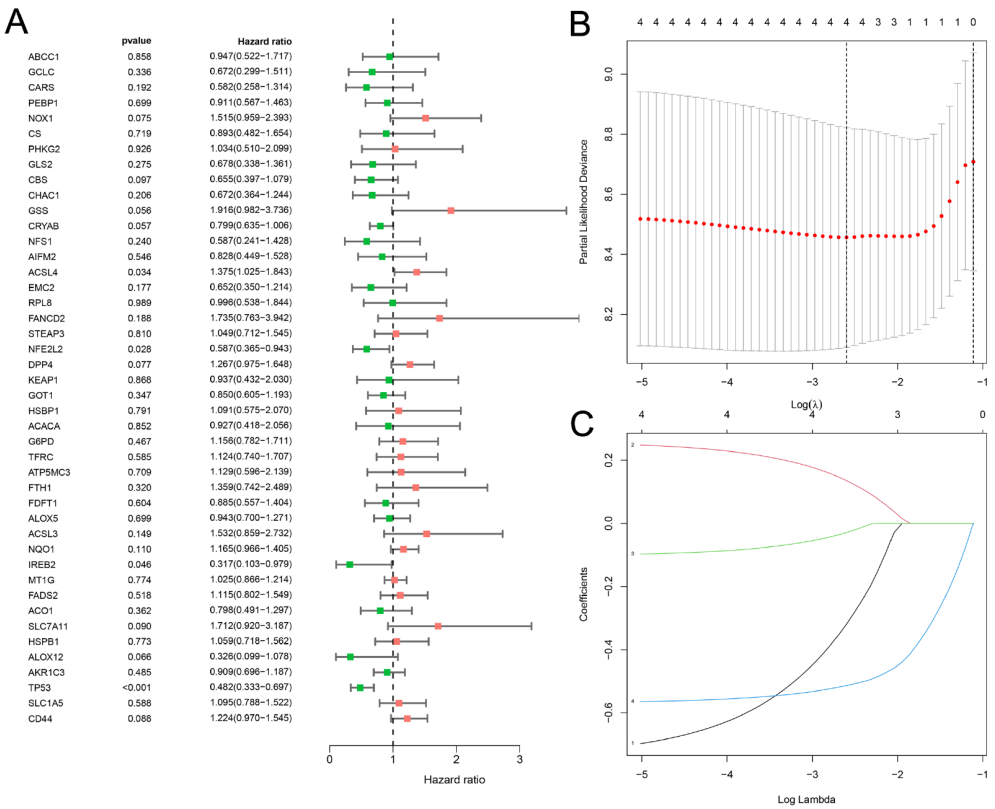

Figure 4. Results of univariate cox regression and LASSO regression analysis in TCGA and GEO cohort (A) Forest plots of univariate cox regression analysis between gene expression and OS. (B) LASSO deviance profiles. (C) LASSO coefficient profiles.

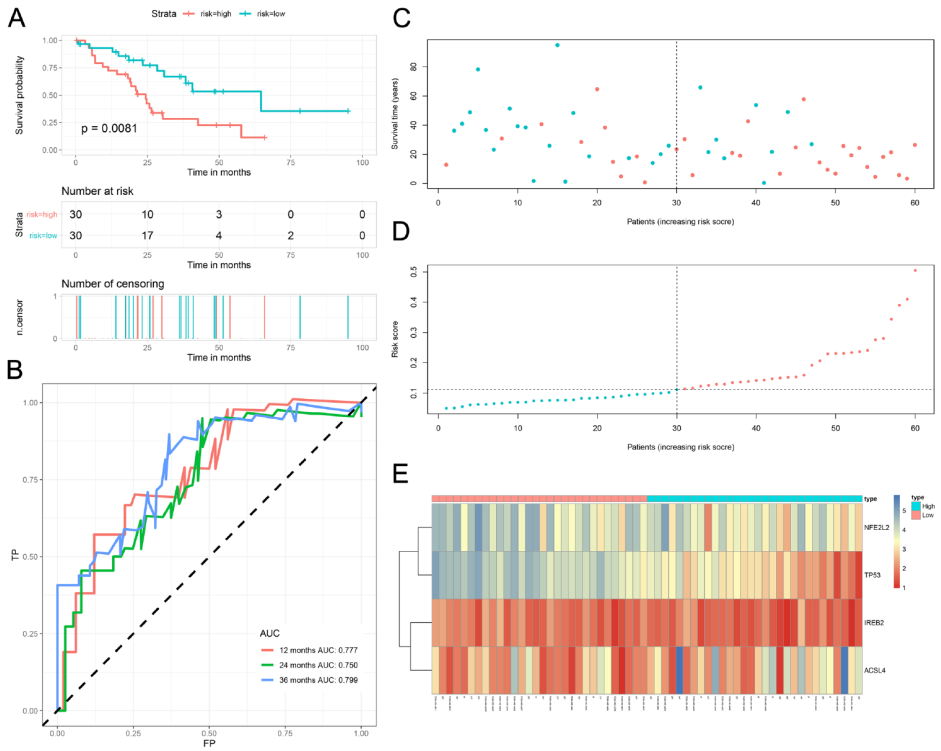

Figure 5. Construction of four ferroptosis-related gene signature in TCGA and GEO cohort (A) Kaplan–Meier curves of OS in the high- and low-risk groups based on the gene signature. (B) AUC of time-dependent ROC curves for 12 months, 24 months and 36 months respectively. (C) Survival status of patients in high-risk and low-risk group. (D) Distribution of patients based on the risk score. (E) The heat-map of the expression levels of ACSL4, IREB2, NFE2L2, TP53 in the low- and high-risk groups in TCGA and GEO cohort.

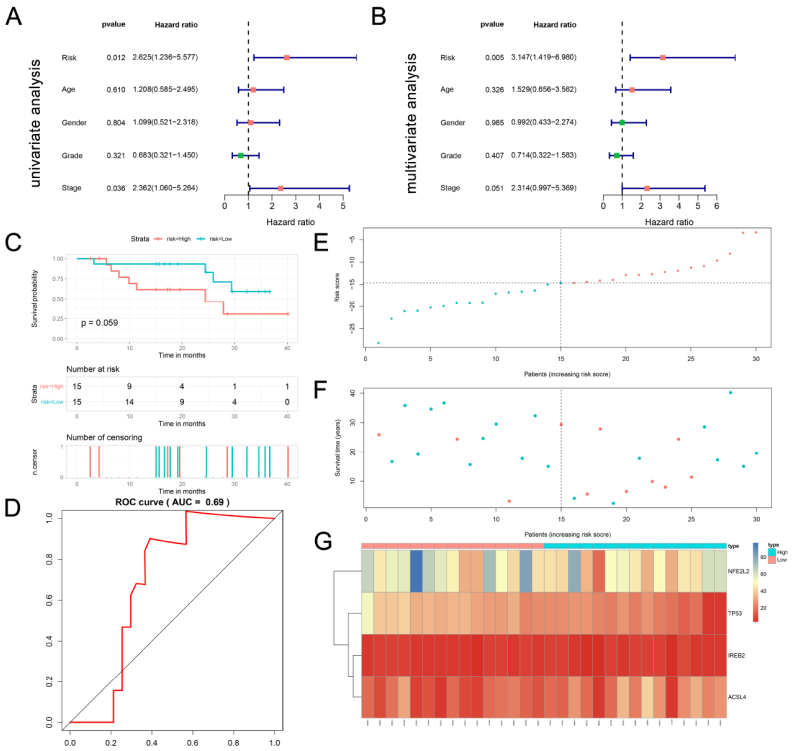

Figure 6. Independent and external validation of four ferroptosis-related gene signature (A) Forest plots of univariate cox analysis. (B) Forest plots of multivariate cox analysis. (C) Kaplan–Meier curves of OS in the high- and low-risk groups based on the gene signature in the WMU cohort. (D) AUC of the time-dependent ROC curve. (E) Distribution of patients based on the risk score; (F) Survival status of patients based on the risk score. (G) The heat-map of the expression levels of ACSL4, IREB2, NFE2L2, TP53 in the low- and high-risk groups in WMU cohort.

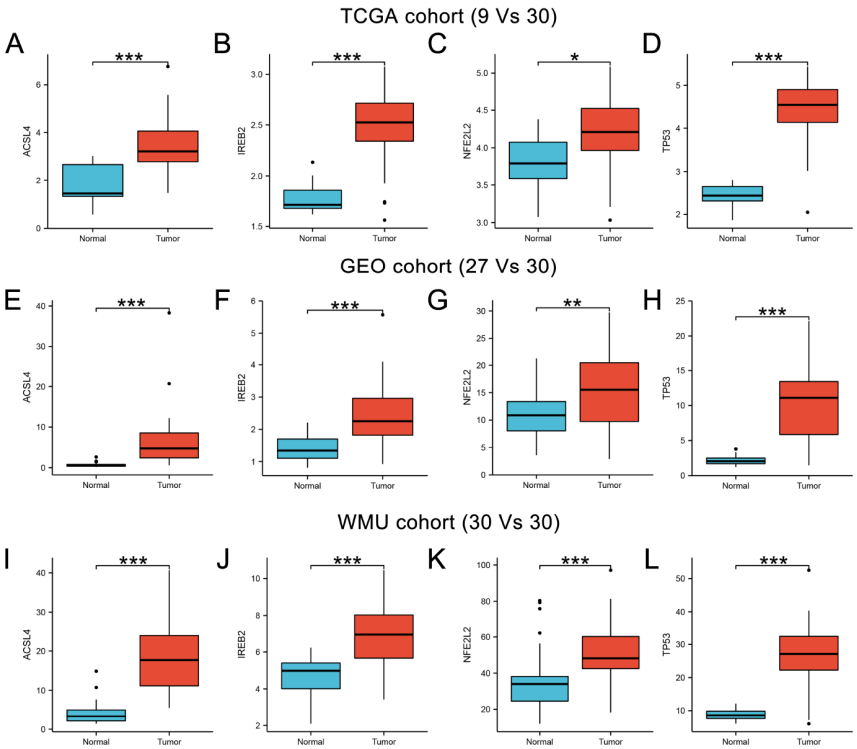

Figure 7. Different expression levels of four ferroptosis-related genes related to the prognosis in three independent cohorts (A–D) Expression of ACSL4, IREB2, NFE2L2, TP53 in TCGA cohort (9 adjacent tissues, 30 tumor tissues). (E–H) Expression of ACSL4, IREB2, NFE2L2, TP53 in GEO cohort (27 adjacent tissues, 30 tumor tissues). (I–L) Expressions of ACSL4, IREB2, NFE2L2, TP53 in WMU cohort (30 adjacent tissues, 30 tumor tissues). $*P<0.05$, $**P<0.01$, $***P<0.001$.

ICC.

Furthermore, we verified the predictive value of the ferroptosis-related gene signature in our own cohort. We built the WMU cohort by collecting the tissue and clinical information of ICC patients who underwent radical surgery in our hospital. Then, we performed transcriptome sequencing analysis to identify the expression of ferroptosis-related DEGs. We found that the expression of ferroptosis-related genes was in accordance with that of the TCGA and GEO cohorts. The patients in the WMU cohort can be divided into a high-risk group and a low-risk group according to the risk score, and the survival time of patients in the high-risk group seemed shorter than that in the low-risk group. Interestingly, although the patients in the high-risk group had a distinctly worse OS than those in the low-risk group according to the KM curve (Figure 6C), the *P* value was 0.059. We speculated that this may be due to the small number of patients enrolled in the study. Subsequent ROC curve analysis further demonstrated the predictive value of the ferroptosis-related gene signature (AUC = 0.69). All these findings may provide new insight into the prediction and prognosis of ICC.

There are also some limitations in our study. First, the samples obtained from the three cohorts (TCGA cohort, GEO cohort, WMU cohort) were small because of the low incidence of ICC. Second, although the ferroptosis-related gene signature was constructed and validated in the three cohorts, the mechanism by which ferroptosis-related genes affect prognosis needs further investigation. Finally, all the information used in the study was acquired from retrospective data, and more prospective real-world data are required to confirm the predictive value of the gene signature.

In conclusion, we established a new predictive model based on four ferroptosis-related genes (*ACSL4*, *IREB2*, *NFE2L2*, and *TP53*) that showed favorable prognostic value in the three cohorts. This study may provide new insight into the prediction and treatment of ICC.

Supplementary Data

Supplementary data is available at *Acta Biochimica et Biophysica Sinica* online.

Funding

This study was supported by the grants from the 2021 National Innovation Project of College Students in China (No. 202110343019), and the 2020 Science and Technology Innovation Activity Plan for Students in Zhejiang Province (No. 2020R413022).

Conflict of Interest

The authors declare that they have no conflict of interest.

References

1. Banales JM, Marin JJG, Lamarca A, Rodrigues PM, Khan SA, Roberts LR, Cardinale V, *et al.* Cholangiocarcinoma 2020: the next horizon in mechanisms and management. *Nat Rev Gastroenterol Hepatol* 2020, 17: 557–588
2. Bertuccio P, Malvezzi M, Carioli G, Hashim D, Boffetta P, El-Serag HB, La Vecchia C, *et al.* Global trends in mortality from intrahepatic and extrahepatic cholangiocarcinoma. *J Hepatol* 2019, 71: 104–114
3. Banales JM, Cardinale V, Carpino G, Marzioni M, Andersen JB, Invernizzi P, Lind GE, *et al.* Cholangiocarcinoma: current knowledge and future perspectives consensus statement from the European Network for the Study of Cholangiocarcinoma (ENS-CCA). *Nat Rev Gastroenterol Hepatol* 2016, 13: 261–280
4. Mazzaferro V, Gorgen A, Roayaie S, Droz Dit Busset M, Sapisochin G. Liver resection and transplantation for intrahepatic cholangiocarcinoma. *J Hepatol* 2020, 72: 364–377
5. Lamarca A, Barriuso J, McNamara MG, Valle JW. Molecular targeted therapies: Ready for "prime time" in biliary tract cancer. *J Hepatol* 2020, 73: 170–185
6. Dixon SJ, Lemberg KM, Lamprecht MR, Skouta R, Zaitsev EM, Gleason CE, Patel DN, *et al.* Ferroptosis: an iron-dependent form of nonapoptotic cell death. *Cell* 2012, 149: 1060–1072
7. Hassannia B, Vandenabeele P, Vanden Berghe T. Targeting ferroptosis to iron out cancer. *Cancer Cell* 2019, 35: 830–849
8. Hangauer MJ, Viswanathan VS, Ryan MJ, Bole D, Eaton JK, Matov A, Galeas J, *et al.* Drug-tolerant persister cancer cells are vulnerable to GPX4 inhibition. *Nature* 2017, 551: 247–250
9. Tang D, Chen X, Kang R, Kroemer G. Ferroptosis: molecular mechanisms and health implications. *Cell Res* 2021, 31: 107–125
10. Doll S, Proneth B, Tyurina YY, Panzilius E, Kobayashi S, Ingold I, Irmler M, *et al.* ACSL4 dictates ferroptosis sensitivity by shaping cellular lipid composition. *Nat Chem Biol* 2017, 13: 91–98
11. Sun X, Ou Z, Chen R, Niu X, Chen D, Kang R, Tang D. Activation of the p62-Keap1-NRF2 pathway protects against ferroptosis in hepatocellular carcinoma cells. *Hepatology* 2016, 63: 173–184
12. Stockwell BR, Friedmann Angeli JP, Bayir H, Bush AI, Conrad M, Dixon SJ, Fulda S, *et al.* Ferroptosis: a regulated cell death nexus linking metabolism, redox biology, and disease. *Cell* 2017, 171: 273–285
13. Bersuker K, Hendricks JM, Li Z, Magtanong L, Ford B, Tang PH, Roberts MA, *et al.* The CoQ oxidoreductase FSP1 acts parallel to GPX4 to inhibit ferroptosis. *Nature* 2019, 575: 688–692
14. Doll S, Freitas FP, Shah R, Aldrovandi M, da Silva MC, Ingold I, Goya Grocin A, *et al.* FSP1 is a glutathione-independent ferroptosis suppressor. *Nature* 2019, 575: 693–698
15. Chen J, Zhan Y, Zhang R, Chen B, Huang J, Li C, Zhang W, *et al.* A new prognostic risk signature of eight ferroptosis-related genes in the clear cell renal cell carcinoma. *Front Oncol* 2021, 11: 700084
16. Roh JL, Kim EH, Jang HJ, Park JY, Shin D. Induction of ferroptotic cell death for overcoming cisplatin resistance of head and neck cancer. *Cancer Lett* 2016, 381: 96–103
17. Yuan Y, Cao W, Zhou H, Qian H, Wang H. CLTRN, regulated by nrf1/ran/dld protein complex, enhances radiation sensitivity of hepatocellular carcinoma cells through ferroptosis pathway. *Int J Radiat Oncol Biol Phys* 2021, 110: 859–871
18. Zhang ZJ, Huang YP, Li XX, Liu ZT, Liu K, Deng XF, Xiong L, *et al.* A novel ferroptosis-related 4-gene prognostic signature for cholangiocarcinoma and photodynamic therapy. *Front Oncol* 2021, 11: 747445
19. Li D, Liu S, Xu J, Chen L, Xu C, Chen F, Xu Z, *et al.* Ferroptosis-related gene CHAC1 is a valid indicator for the poor prognosis of kidney renal clear cell carcinoma. *J Cell Mol Medi* 2021, 25: 3610–3621
20. Liu Y, Zhang X, Zhang J, Tan J, Li J, Song Z. Development and validation of a combined ferroptosis and immune prognostic classifier for hepatocellular carcinoma. *Front Cell Dev Biol* 2020, 8: 596679
21. Wang Z, Zhang Y, Chen Y, Liu S, Li C, Li X. Identification of a ferroptosis-related gene signature for predicting the prognosis of cholangiocarcinoma. *Expert Rev Gastroenterol Hepatol* 2022, 16: 181–191
22. Liao P, Wang W, Wang W, Kryczek I, Li X, Bian Y, Sell A, *et al.* CD8+ T cells and fatty acids orchestrate tumor ferroptosis and immunity via ACSL4. *Cancer Cell* 2022, 40: 365–378.e6
23. Yu Y, Sun X, Chen F, Liu M. Genetic alteration, prognostic and immunological role of acyl-coa synthetase long-chain family member 4 in a

pan-cancer analysis. *Front Genet* 2022, 13: 812674
24. Tang X, Ding H, Liang M, Chen X, Yan Y, Wan N, Chen Q, *et al.* Curcumin induces ferroptosis in non-small-cell lung cancer via activating autophagy. *Thorac Cancer* 2021, 12: 1219–1230
25. Liu Z, Lv X, Song E, Song Y. Fostered Nrf2 expression antagonizes iron overload and glutathione depletion to promote resistance of neuron-like cells to ferroptosis. *Toxicol Appl Pharmacol* 2020, 407: 115241
26. Yi K, Liu JC, Rong Y, Wang C, Tang X, Zhang XP, Xiong Y, *et al.* Biological functions and prognostic value of ferroptosis-related genes in bladder cancer. *Front Mol Biosci* 2021, 8: 631152
27. Kang R, Kroemer G, Tang D. The tumor suppressor protein p53 and the ferroptosis network. *Free Radical Biol Med* 2019, 133: 162–168